Knee Surg Sports Traumatol Arthrosc (2012) 20:1192–1204
DOI 10.1007/s00167-011-1692-9

EXPERIMENTAL STUDY

A novel nano-structured porous polycaprolactone scaffold improves hyaline cartilage repair in a rabbit model compared to a collagen type I/III scaffold: in vitro and in vivo studies

Bjørn Borsøe Christensen · Casper Bindzus Foldager · Ole Møller Hansen · Asger Albæk Kristiansen · Dang Quang Svend Le · Agnete Desirée Nielsen · Jens Vinge Nygaard · Cody Erik Bünger · Martin Lind

Received: 11 May 2011 / Accepted: 20 September 2011 / Published online: 5 October 2011

Abstract
Purpose To develop a nano-structured porous polycaprolactone (NSP-PCL) scaffold and compare the articular cartilage repair potential with that of a commercially available collagen type I/III (Chondro-Gide®) scaffold.
Methods By combining rapid prototyping and thermally induced phase separation, the NSP-PCL scaffold was produced for matrix-assisted autologous chondrocyte implantation. Lyophilizing a water–dioxane–PCL solution created micro and nano-pores. In vitro: The scaffolds were seeded with rabbit chondrocytes and cultured in hypoxia for 6 days. qRT–PCR was performed using primers for sox9, aggrecan, collagen type 1 and 2. In vivo: 15 New Zealand White Rabbits received bilateral osteochondral defects in the femoral intercondylar grooves. Autologous chondrocytes were harvested 4 weeks prior to surgery. There were 3 treatment groups: (1) NSP-PCL scaffold without cells. (2) The Chondro-Gide® scaffold with autologous chondrocytes and (3) NSP-PCL scaffold with autologous chondrocytes. Observation period was 13 weeks. Histological evaluation was made using the O'Driscoll score.
Results In vitro: The expressions of sox9 and aggrecan were higher in the NSP-PCL scaffold, while expression of collagen 1 was lower compared to the Chondro-Gide® scaffold. In vivo: Both NSP-PCL scaffolds with and without cells scored significantly higher than the Chondro-Gide® scaffold when looking at the structural integrity and the surface regularity of the repair tissue. No differences were found between the NSP-PCL scaffold with and without cells.
Conclusion The NSP-PCL scaffold demonstrated higher in vitro expression of chondrogenic markers and had higher in vivo histological scores compared to the Chondro-Gide® scaffold. The improved chondrocytic differentiation can potentially produce more hyaline cartilage during clinical cartilage repair. It appears to be a suitable cell-free implant for hyaline cartilage repair and could provide a less costly and more effective treatment option than the Chondro-Gide® scaffold with cells.

Keywords Chondrocyte transplantation · Cell-free scaffold · Articular cartilage repair · Rabbit model · Polycaprolactone

B. B. Christensen (✉) · C. B. Foldager · O. M. Hansen · C. E. Bünger
Orthopaedic Research Laboratory, Aarhus University Hospital, Nørrebrogade 44, Build. 1A, 1. Floor, 8000 Aarhus C, Denmark
e-mail: bjornbc@gmail.com

A. A. Kristiansen · D. Q. S. Le · J. V. Nygaard
Interdisciplinary Nanoscience Center, Aarhus University, Ny Munkegade 120, 8000 Aarhus C, Denmark

A. D. Nielsen
Department of Radiology, Silkeborg Regional Hospital, Falkevej 1-3, 8600 Silkeborg, Denmark

M. Lind
Department of Orthopaedic Surgery, The Sports Trauma Clinic, Aarhus University Hospital, Tage Hansens Gade 2, 8000 Aarhus C, Denmark

Introduction

Due to the avascular nature of articular cartilage, injuries to this tissue have shown a limited potential to regenerate [5]. Cartilage defects in the knee may cause pain, swelling and lead to early development of osteoarthritis [13, 30]. Current treatment methods include Pridie drilling, debridement, microfracture, autologous matrix-induced chondrogenesis

(AMIC), mosaic plasty, autologous chondrocyte implantation (ACI) and matrix-induced autologous chondrocyte implantation (MACI), but a gold standard for treatment of articular cartilage injuries is yet to be established [5, 13, 20]. The ACI method was first described in a clinical setting in 1994 by Brittberg et al. [4]. In this 1st generation ACI procedure, a cartilage biopsy is taken from the patient and cultured. At a subsequent procedure, the chondrocytes are injected into the cartilage defect under a ceiled periosteal flap cover.

Because the use of a periosteal membrane, often resulted in repair tissue hypertrophy, collagen-based synthetic membranes have widely replaced the periosteal cover in the 2nd generation ACI [2, 15]. One of the most clinically used collagen membranes is a porcine collagen type I/III scaffold (Chondro-Gide® Geistlich Biomaterials, Wolhusen, Switzerland). The porcine collagen type I/III scaffold is being used in the AMIC technique, which is a membrane-covered microfracture technique, where the collagen membrane is sutured onto the defect in order to contain the blood clot and mesenchymal stem cells [3]. In addition, the scaffold is used in the before mentioned 2nd generation ACI [9, 23] and finally in the 3rd generation ACI technique [or matrix-assisted ACI (MACI)], where autologous chondrocytes are seeded onto a three-dimensional scaffold, which is then press fitted or glued into the defect [1, 14]. Results using the Chondro-Gide® scaffold have been diverse. Haddo et al. [9] found their clinical outcome to be satisfactory and without evidence of hypertrophy at 1-year arthroscopy as compared to periosteum. However, in a comparative study by Niemayer et al. [23], the use of Chondro-Gide® resulted in reoperation of 12.1% of the cases within 20 months, and in a study by Russlies et al. [28], the repair tissue of the Chondro-Gide® scaffold was found not to be biomechanically comparable to genuine articular cartilage.

Polycaprolactone (PCL) is one of the most widely used biodegradable polyesters for medical application due to its slow biodegradability, biocompatibility, mechanical properties and structural flexibility [22]. PCL express slow degradation kinematics and its degradation products are harmlessly metabolized in the tricarboxylic acid cycle [26, 31]. PCL-based scaffolds have shown to have a potential for cartilage repair [12, 21, 29]. Martinez-Diaz et al. [19] found that osteochondral defects treated with a PCL scaffold had a good integration in the subchondral bone and the surrounding cartilage. Furthermore, indentation tests showed that the PCL aided repair tissue had stress–strain curves similar to that of normal articular cartilage. In order to combine the mechanical stability of the PCL scaffold with a large porous surface area for cell attachment, we developed a novel scaffold type (patent application# EP09163896.5). It is a nano-structured porous PCL (NSP-PCL) scaffold that expresses both macro-, micro and nano-pores to benefit mechanical strength, cell adherence, viability and metabolism. The scaffold was constructed using fused deposition modeling (FDM), a rapid prototyping technique where 3-D shapes can be printed to specific shapes and sizes to fit into a designated area. The manufacturing technique allows for the scaffold to be created in any shape or size, which could potentially be done from an MRI scan of the injured area.

The novel NSP-PCL scaffold holds several hypothetical advantages over existing scaffolds. The unique combination of a plotted and a lyophilized structure makes the scaffold highly resistible to pressure, while maintaining a large surface area for cells to adhere. In addition, rapid prototyping is a fast, specific and low-cost method, and the plotted scaffolds hold the potential of future functionalization with growth and differentiation factors or siRNA.

The aim of this study was to compare the hyaline cartilage regenerative ability of the novel NSP-PCL scaffold with autologous cells, the NSP-PCL scaffold without cell and the clinically used Chondro-Gide® scaffold with autologous cells. The hypothesis was that the combination of the nano-structure and the mechanical stability of the NSP-PCL scaffolds can be used for cartilage repair and is comparable with clinically used materials such as Chondro-Gide®.

Materials and methods

Scaffolds

The NSP-PCL scaffolds were constructed by a BioScaffolder (SYS + ENG, Germany). PCL fibers [molecular weight (MW) 50 kDa] with a diameter of 120 μm were deposited producing a 3-D web. The scaffold was subsequently submerged into in a mixture of dioxane, PCL (MW 25 kDa) and water. It was then phase separated creating macro-, micro and nano-pores (Fig. 1a, b). Based on yet unpublished data, the water/dioxane ratio creating the most optimal micro and nano-structure was selected. Using a 4 mm skin biopsy punch, the scaffolds were punched out from a 2 mm high sheet forming a cylinder, 4 mm in diameter.

The scaffolds were sterilized in vacuum using ethanol concentrations of 96, 70 and 50%, and sterile H_2O, each for 30 min. To increase surface hydrophilicity, the scaffolds were treated with 1.25 M NaOH for 16 h, neutralized in 1 M HCl for 1 h and rinsed in sterile H_2O.

The Chondro-Gide® (Geistlich Group, Switzerland) scaffolds consist of porcine collagen type I and type III. One side consists of a porous layer with collagen fibers in a loose, open weave arrangement that is designed to favor cell invasion and attachment, while the other side consists of a compact membrane layer that is cell occlusive [7].

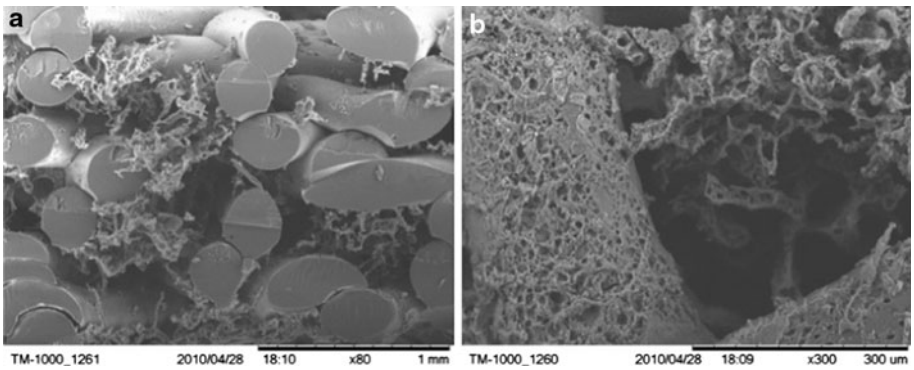

Fig. 1 **a** A SEM image of the NSP-PCL scaffold cut sagitally (Zoom ×80). **b** A SEM image of the lyophilized structure of the NSP-PCL scaffold, showing the macro- and micropores (Zoom ×300)

Cartilage biopsies and isolation of chondrocytes

The rabbits were anesthetized by an intramuscular injection of 40 mg (13.3 mg/kg) xylazine and 150 mg (50 mg/kg) *S*-ketamine to provide a surgical anesthesia lasting approximately 1 h. Using sterile techniques, a medial parapatellar arthrotomy was performed and the patella was laterally displaced. A biopsy of the cartilage was taken from the proximal non-load bearing part of the knee, the articular capsule and the skin were sutured and the rabbits were returned to their cages and allowed free cage activity. Postoperative analgesia consists of fentanyl (Matrifen, Roskilde, DK; 0.0015 mg/kg/h) on the day of the surgery. The biopsies were transported to the laboratory facility in a suspension of DMEM/F-12 with Glutamax (Gibco-Invitrogen), 10% FCS, streptomycin and penicillin (Sigma–Aldrich). Each biopsy was digested using 0.1% collagenase II (Gibco) and 0.1% hyaloronidase (Sigma–Aldrich) for 18–20 h in 37°C in a water bath. The cells were washed in DMEM/F-12 (Gibco–Invitrogen) and seeded in a T25 flask (Techno Plastic Products AG) in standard culture media containing 10% FCS and the antibiotics mentioned above. The cells were cultured in a humidified atmosphere of 5% CO_2 at 37°C and were subsequently fed continuously by replacing the growth medium every 3–4 days until 70–80% confluence had been reached. After 3 weeks in culture, ex vivo expanded chondrocytes of passages 1 or 2 were detached by trypsin/EDTA treatment. Six days prior to in vivo implantation, 105,000 chondrocytes suspended in 10 µl of media (10.5×10^6 cells/ml) were seeded onto the pre-wetted NSP-PCL and Chondro-Gide® scaffolds. The scaffolds were left in the incubator for 2 h to allow the cells to adhere to the scaffold, followed by a careful addition of 1 ml of optimized growth medium DMEM/F12. The scaffolds were cultured in hypoxia (5% oxygen tension) before being implanted into the defect. In addition, 30 NSP-PCL scaffolds and 30 Chondro-Gide® scaffolds were seeded with the rabbit chondrocytes for the in vitro investigations described later.

The scaffolds in group 1 (NSP-PCL/empty) were treated similarly to the scaffolds in groups 2 and 3, apart from cell seeding.

In vitro investigations with real-time quantitative polymerase chain reaction (qRT–PCR)

The 30 NSP-PCL scaffolds and 30 Chondro-Gide® scaffolds were placed in 24-well plates coated with a 1% agarose gel to prevent cells from adhering to the well walls. As described in the previously, the scaffolds were pre-wetted in an incubator with a humidified atmosphere of 5% CO_2 at 37°C for 2 h and seeded with the rabbit chondrocytes, with a cell seeding density of 105,000 cells per scaffold, suspended in 10 µl of media. The scaffolds were cultured in hypoxia (5% oxygen tension) for 6 days before being treated/lyzed according to the GenElute Mammalian Total RNA Miniprep Kit User Guide (Sigma-Aldrich). After the purified RNA was obtained, it was quantified by the QuantiT RiboGreen RNA Kit (Molecular Probes), and DNase I treated (Ambion, Cambridgeshire, UK) before being converted to complementary DNA (cDNA) and qRT–PCR was performed on a 7500 Fast Real–Time PCR system (Applied Biosystems, Naerum, Denmark) using primers for sox9 (Assay ID: Oc04096872_m1), aggrecan, collagen type 1 (Assay ID: Oc03396073_g1) and collagen type 2. The housekeeping genes 36B4 (Assay ID: Oc03396140_g1) and GAPDH were selected based on BestKeeper evaluation [25].

The sox9, collagen type 1 and 36B4 assays were purchased from Applied Biosystems (TaqMan GENE Expression assays). The two unlabeled primers and the FAM dye-labeled TaqMan MGB probe used for every gene were designed using the Applied BioSystems Primer Express 3.0 software. The details are specified in Table 1. To verify the predicted size of the PCR amplicon and to check that only one product was being amplified, the PCR products for every gene were tested by electrophoresis in agarose gels. Furthermore, we used dilution curves of cDNA to verify a good PCR-efficiency.

Table 1 Details of assays produced in our laboratory

Gene symbol	Gene name	Accession number	Forward primer
GAPDH	Glyceraldehyde-3-phosphate dehydrogenase	NM_001082253	GGATTTGGCCGCATTGG
Coll II	Pro alpha1 type II collagen	S83370	AGGGCCCGTCTGCTTCTT
AGC	Aggrecan	L38480	TTCCCTGGCGTGAGAACCT

Reverse primer	FAM™ dye-labeled TaqMan® MGB probe	Amplicon size (bp)
ACAACATCCACTTTGCCAGAGTT	TCACCAGGGCTGCTT	65
GAGCACTCGGGTCCTTTGG	AAGCCGAGCTCTGAACA	59
GCGAAGCAGTACACGTCATAGG	CCGGGACACCAACG	65

Experimental design

Fifteen mature male New Zealand White Rabbits were used. The rabbits were 6 months old and each weighed approximately 3 kg. All 15 animals were operated on both knees, giving a total of 30 knees treated. All animal surgeries and in vitro experiments complied with the Danish Law on Animal Experimentation and were approved by the Danish Ministry of Justice Ethical Committee, J.nr. 2008-561-1459. Each rabbit knee was randomized into one of the three treatment groups. The groups were as follows: Group 1: NSP-PCL scaffold without cells (NSP-PCL/empty), Group 2: The Chondro-Gide® scaffold with autologous chondrocytes (CG) and Group 3: NSP-PCL scaffold with autologous chondrocytes (NSP-PCL/cells). Each group consisted of ten rabbit knees. One sample from group 2 and one from group 3 was lost during the preparation for histology.

Surgery

The rabbits were anaesthetized as described in the "cartilage biopsies" paragraph. After anesthesia, the knee joints were shaven and the rabbits were placed in a supine position and prepared for the sterile procedure. An anteromedial incision of approximately 3 cm was made, and after gaining access to the knee joint, the patella was retracted laterally. An osteochondral defect was made in the interchondylar groove of the femur using a Ø 4 mm steel drill. Drilling was performed to a depth of 3 mm. The defect was cleaned with a non-traumatic forceps. The NSP-PCL scaffold was press fitted into the drill hole and glued in place with fibrin glue (Tisseel Duo Quick, Baxter, Vienna, Austria). The Chondro-Gide® scaffold was placed in the defect, and the glue was carefully applied along the edge of the scaffold. The glue was allowed to set, and patella was temporarily repositioned in order to bend and stretch the leg. The patella was subsequently retracted, and the defect containing the scaffold was examined to ensure that the scaffold was still in place. The articular capsule and the skin were sutured, and the rabbits were returned to their cages and allowed free cage activity. Postoperative analgesia consists of fentanyl (patch) (Matrifen, Roskilde, DK; 0.0015 mg/kg/h) on the day of the surgery.

Follow up

The rabbits were housed individually with free access to water. Postoperative analgesic fentanyl (Matrifen, Roskilde, DK; 0.0015 mg/kg/h) was administrated for 3 days. Thirteen weeks postoperatively, the rabbits were sacrificed by an intracardial injection of pentobarbital (100 mg/kg) under general anesthesia as described in the "cartilage biopsies" paragraph.

Histology

The resected distal femur was stripped of soft tissue and dehydrated in a graded series of ethanol (70–96%). It was cleared in xylene and embedded in methylmetacrylate (MMA). Using a microtome, (Polycut E, Reichert-Jung, Heidelberg, Germany) eight slices, with a thickness of 7 μm, were made on three different levels of the defect. Level 1 was in the periphery of the defect, and level 3 was in the center (Fig. 2). All the samples were cut in a random direction perpendicular to the surface plane. The samples were stained with safranin-*O*, hematoxylin-eosin (HE), collagen 2 antibody staining and collagen 1 antibody

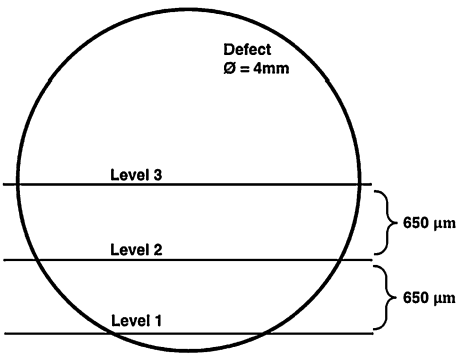

Fig. 2 A schematic drawing of how the defects were cut for histology

staining. Scoring of cartilage quality was performed blindly using the validated O'Driscoll semiquantitative microscopic system, grading the samples using 9 categories: cellular morphology, safranin-*O* staining of the matrix, surface regularity, structural integrity, thickness of the regenerated cartilage, bonding to adjacent cartilage, level of hypocellularity, level of chondrocyte clustering and freedom from degenerative changes in adjacent cartilage. The maximal achievable total score was 24 points [24].

Statistical analysis

All data were analyzed using STATA (StataCorp, College Station, Texas, USA). The qRT–PCR data were ln-transformed and residuals were checked for normal distribution using QQ-plots. The data were analyzed using one-way ANOVA. The non-parametric histological data were analyzed using a Kruskal–Wallis equality-of-populations rank test to determine differences in mean value. The groups were then compared using the χ^2 test. P values < 0.05 were considered significant.

Results

In vitro study gene expression

The results of the qRT–PCR are shown in Fig. 3. The relative expression to the housekeeping genes, of the chondrogenic markers sox9 ($P < 0.001$) and aggrecan ($P < 0.001$), was higher in the NSP-PCL scaffold than in the Chondro-Gide® scaffold, and the fibrous tissue marker collagen type 1 was lower in the NSP-PCL scaffold than in the Chondro-Gide® scaffold ($P < 0.001$). Although the collagen type 2 expressions were higher in the NSP-PCL scaffolds, the difference was not significant.

Macroscopic evaluation

Macroscopically, the defects treated with the NSP-PCL/cells (group 3) and the NSP-PCL/empty (group 1) appeared roughly the same (Fig. 4a, b). In all 10 knees of both groups 1 and 3, the defects were clearly outlined and the color of the repair tissue was different from the surrounding tissue; however, the surface seemed smooth and well integrated with the neighboring tissue. The macroscopic appearance of the defects treated with the Chondro-Gide® scaffold demonstrated a large variation within the treatment group. In 7 of 10 knees, there was a large unfilled hole in the defect (Fig. 4c), while in 3 of 10 knees, the defect appeared almost completely filled (Fig. 4d).

Histology

Visual analysis of the histological cuts

The knees treated with the NSP-PCL scaffolds had a very good filling of the defect (Figs. 5, 6, 7, 8, 9, 10a, b, d, e, g, h). The scaffolds were still in place in all samples, and some bone ingrowth was seen. However, the osteochondral junction was only restored in one sample (Fig. 5a). The scaffold was not visibly degraded. There was a good bonding to the adjacent tissue, and especially the surface regularity and the structural integrity were reestablished

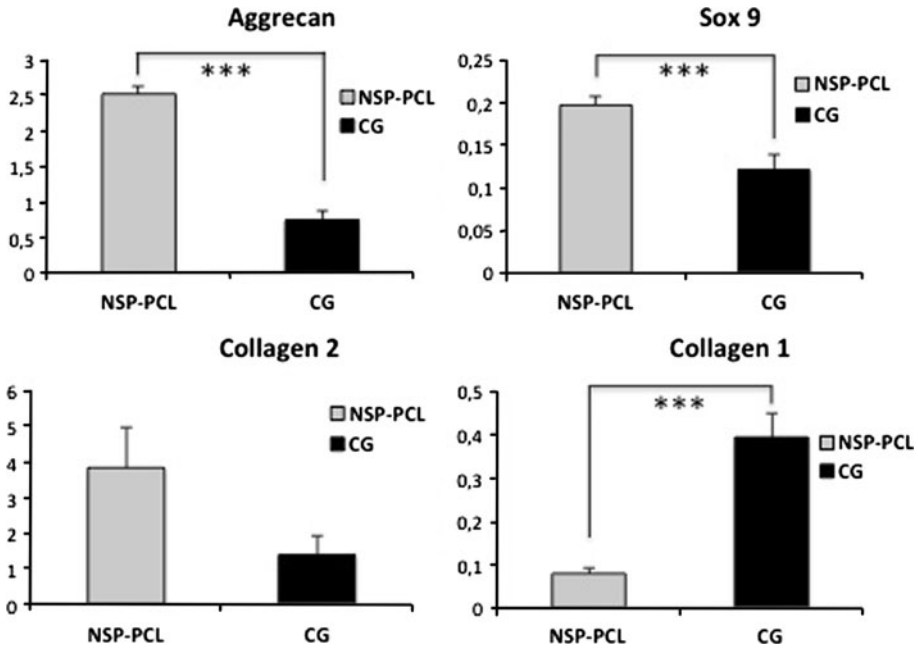

Fig. 3 Relative gene expression levels of the expression of sox9, aggrecan, collagen type 1 and collagen type 2 in the NSP-PCL scaffold (NSP-PCL) and the Chondro-Gide® scaffold (CG). The *Y* axis is the relative gene expression compared to the housekeeping genes. *Error bars* = SEM (***$P < 0.001$; $n = 30$)

Fig. 4 The distal part of the femur 13 weeks after implantation. **a** is treated with NSP-PCL/cells (group 3), **b** is treated with NSP-PCL/empty (group 1), **c** and **d** are treated with CG (group 2), but have very different macroscopic appearance. **c** has a large hole in the *middle* of the defect (*blue arrow*) and **d** appears well healed. The defects are marked with *black arrows*

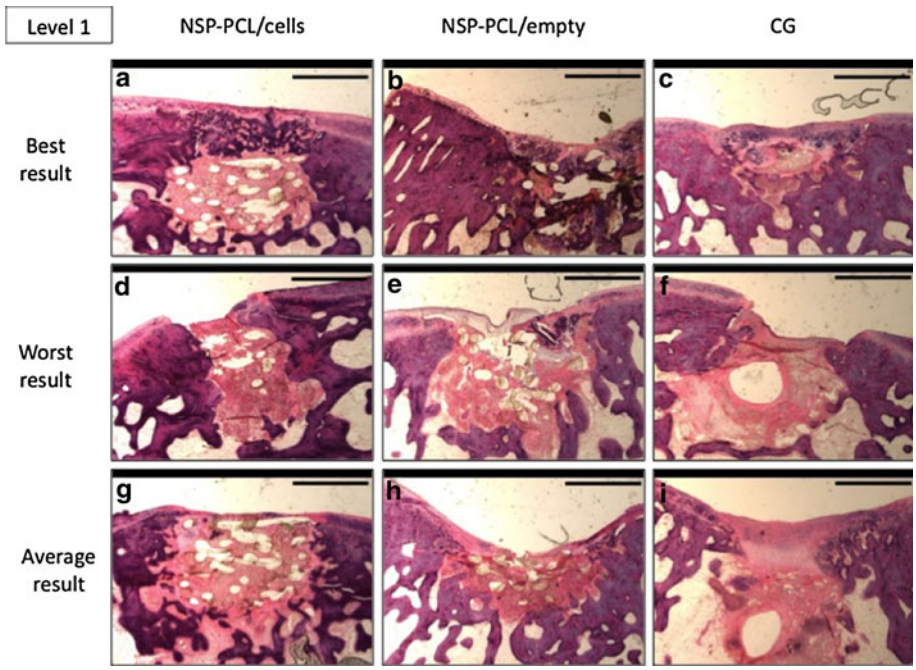

Fig. 5 Best, worst and average histological *images* of the knee defects on level 1. Zoom level is 1.25 and staining is HE. The *black bars* are 1,500 µm. The different appearance of the knees is due to the random direction, orthogonally to the surface, in which they were cut

well. In some samples, the fibers of the scaffold penetrated the surface, and since the histology embedding process removes most of the scaffold fibers, some artifact defects were seen. This was a cause for a lower score in some samples (Fig. 7g).

The defects treated with the Chondro-Gide® scaffold did not appear to be as well filled. In the majority, a large hole was seen in the defect, causing the sample to receive low scores in surface regularity and structural integrity (Figs. 6f, i, 7f, i, 9c, f, i, 10c, f, i). In other samples, a complete restoration of the cartilage surface was seen; however, a large hole had formed beneath the surface, causing the sample to receive low scores in structural integrity (Fig. 5f, i).

Figures 8, 9 and 10a–f show that the articular cartilage tissue was not completely restored in any sample after 13 weeks. Figure 12b and d of the NSP-PCL scaffold with and withoutcells, show what could be the beginning of the zonal stratification seen in mature hyaline cartilage. Figure 11 shows that no zonal stratification is seen in the equivalent zone of a defect treated with the Chondro-Gide scaffold.

Histological scoring

Each sample was scored at cutting levels 1–3 using the O'Driscoll Score. No statistically significant difference was found between NSP-PCL/cells and NSP-PCL/empty on any level of the defect or in any category of scoring. However, both NSP-PCL/cells and NSP-PCL/empty scored higher in total score (adding the scores of the 9 categories and the three levels) than CG ($P = 0.002$) (Fig. 13a). Furthermore, both NSP-PCL/cells and NSP-PCL/empty scored higher than CG in structural integrity on level 1 ($P = 0.013$), 2 ($P = 0.001$) and 3 ($P = 0.001$) (Fig. 13b). On level 2 ($P = 0.0007$) and 3 ($P = 0.002$), both NSP-PCL/cells and NSP-PCL/empty scored higher than CG in surface regularity (Fig. 13c).

Even though no significant difference between the three treatments was found in any other category, a trend was seen to favor of the NSP-PCL scaffolds. Figure 14 shows the total O'Driscoll score on the three levels for the three treatments. The illustration shows that the defects are repaired from the periphery and inwards.

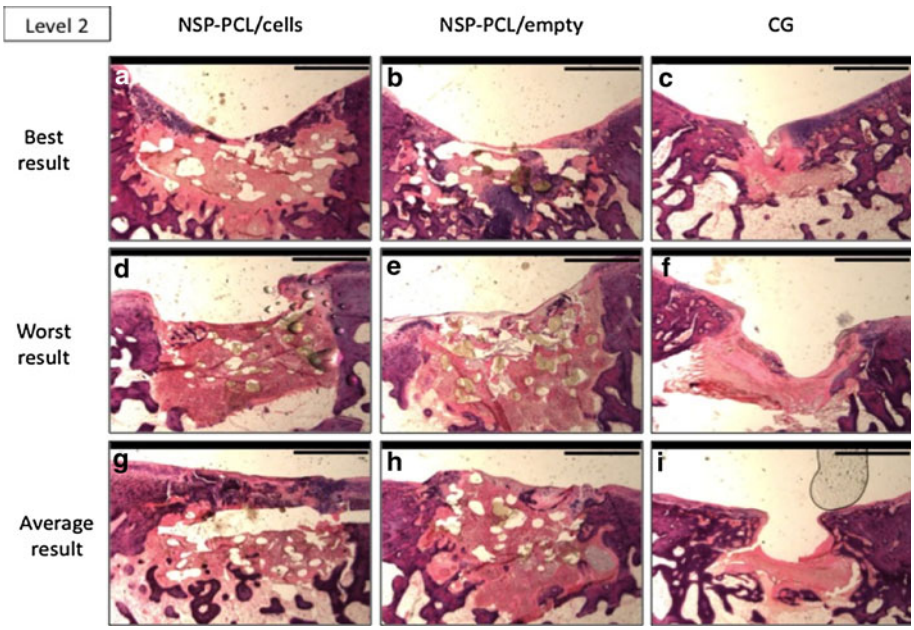

Fig. 6 Best, worst and average histological *images* of the knee defects on level 2. Zoom level is ×1.25 and staining is HE. The *black bars* are 1,500 μm

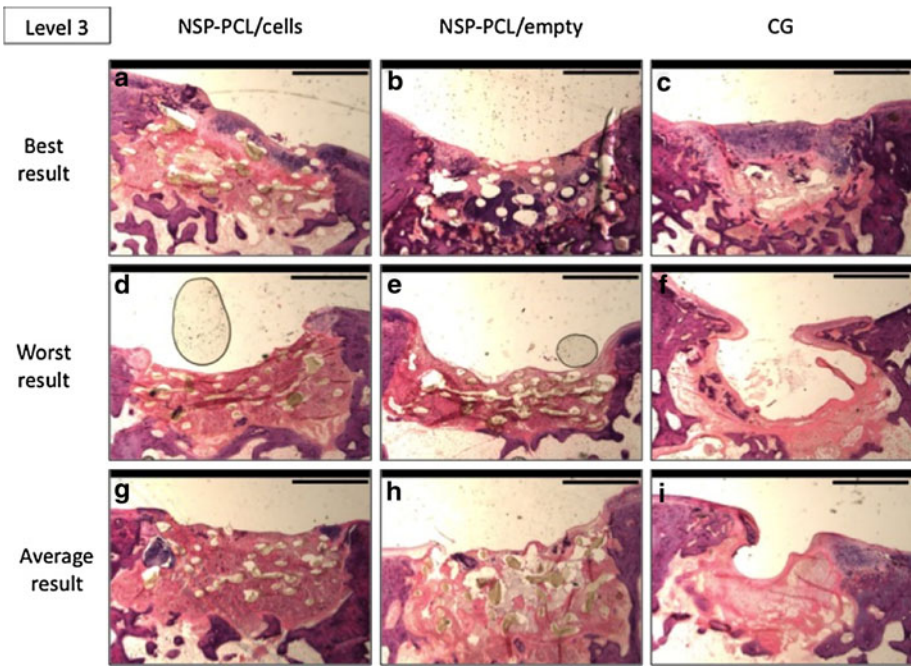

Fig. 7 Best, worst and average histological *images* of the knee defects on level 3. Zoom level is ×1.25 and staining is HE. The *black bars* are 1,500 μm

Discussion

The most important finding of the present study was that the use of the NSP-PCL scaffold, with and without prior cell seeding, led to better histological results when looking at the structural integrity and the surface regularity of the repair tissue than a collagen-based scaffold. This repair response was similar for the NSP-PCL scaffold with and without prior cell seeding. Furthermore, the NSP-PCL scaffold produced a higher expression of the chondrogenic markers sox9 and aggrecan, and a lower expression of the osteogenic/fibrous marker collagen type 1 in an in vitro setting.

The key clinical challenge to cartilage repair techniques is to produce a repair tissue with the correct phenotype of hyaline cartilage. The improved chondrogenic phenotypic response demonstrated in the present study indicates that the NSP-PCL scaffold hold an advantage over existing techniques. Another problem for cartilage repair is the high cost of products that include cultured cells. Since the NSP-PCL scaffold without cells demonstrated better repair response than a collagen scaffold with cells, and similar

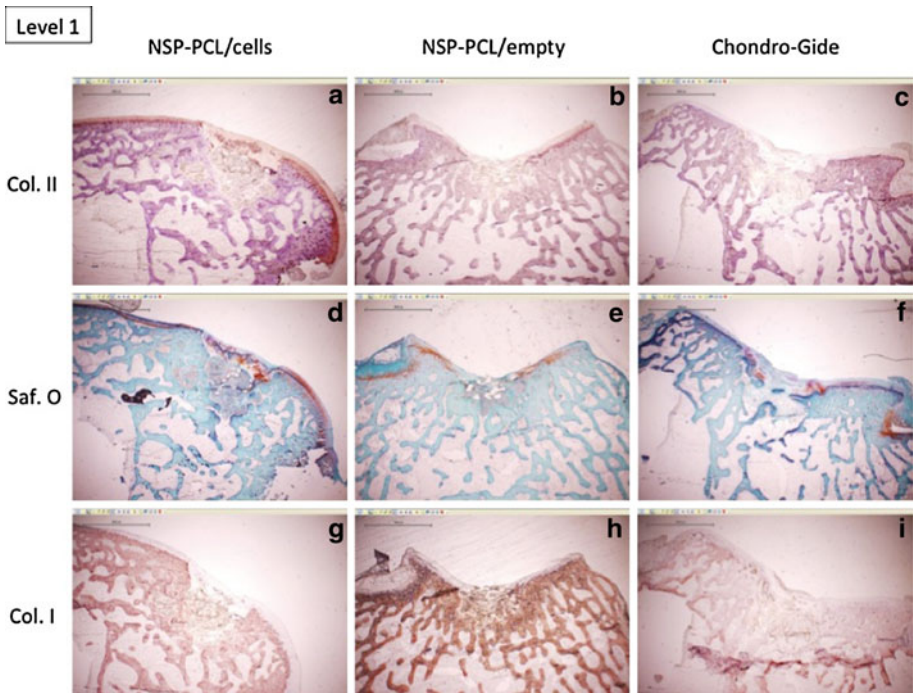

Fig. 8 The average histological results of the three treatment groups on level 1, stained with collagen type 2 antibodies **a**–**c**, safranin-*O* **d**–**f** and collagen type 1 antibodies **g**–**i**. The *bars* in the *top left corner* are 2,500 μm

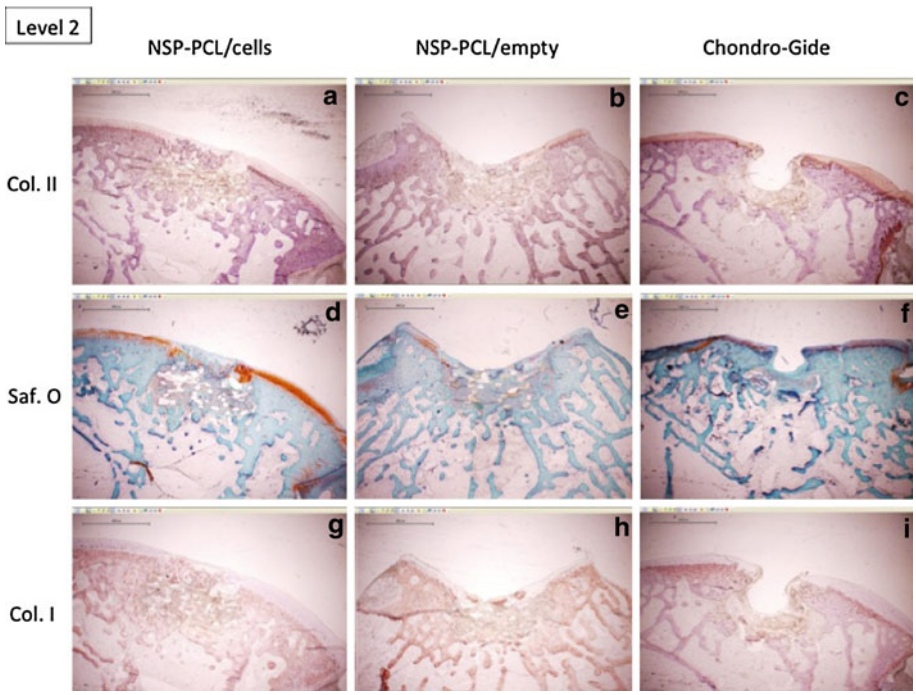

Fig. 9 The average histological results of the three treatment groups on level 2, stained with collagen type 2 antibodies **a**–**c**, safranin-*O* **d**–**f** and collagen type 1 antibodies **g**–**i**. The *bars* in the *top left corner* are 2,500 μm

response to the NSP-PCL scaffold with cells, the scaffold can potentially be used as a cell-free implant which significantly reduced cost.

Sox9 has been found to directly suppress vascular endothelial growth factor type A (VEGFA) expression by binding SRY to the VEGFA gene [11]. VEGFA is important for angiogenesis, and blocking of VEGFA improves articular cartilage repair by preventing vascularization of the tissue [16]. Furthermore, studies suggest that sox9 plays an important role in the suppression of Runt-related transcription factor 2 (RUNX2), a critical enhancer of osteoblasts and possibly an enhancer of the expression of VEGFA [11, 32]. This suggests that the NSP-PCL scaffold has a higher potential than the Chondro-Gide® scaffold for hyaline cartilage development without subsequent vascularization and ossification of the cartilage.

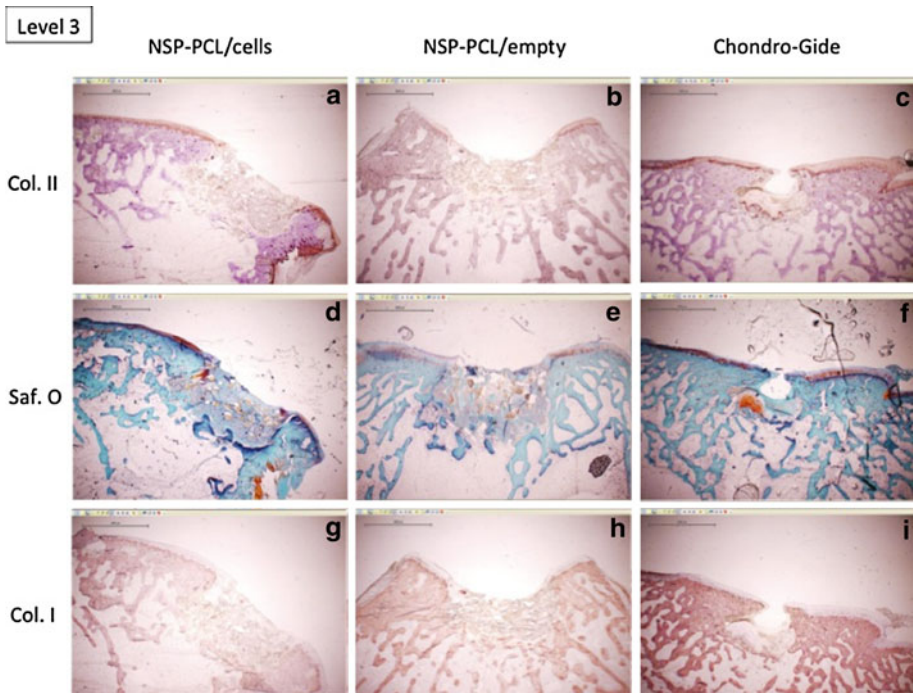

Fig. 10 The average histological results of the three treatment groups on level 3, stained with collagen type 2 antibodies **a–c**, safranin-*O* **d–f** and collagen type 1 antibodies **g–i**. The *bars* in the *top left corner* are 2,500 μm

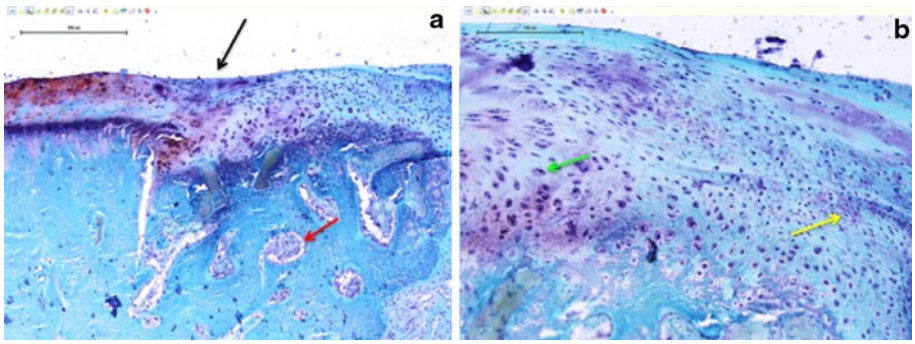

Fig. 11 Chondro-Gide treated knee stained with safranin-*O*. The micrographs are taken from level 3 of the defect. **a** A ×10 magnification of the transition zone (*black arrow*) between healthy cartilage and regenerated tissue. The micrograph shows that although cartilaginous tissue is being formed, no clear hyaline structure is found. The *red arrow* shows the formation of bone by osteoblasts. **b** A ×20 magnification of the *adjacent area*. The *green arrow* shows a chondrocyte, and further away from the healthy cartilage, the *yellow arrow* shows an area of fibroblasts

The higher relative expression of chondrogenic markers aggrecan and collagen type 2 and the lower relative expression of the fibrous tissue marker collagen type 1 in the NSP-PCL scaffold compared to the Chondro-Gide® scaffold (Fig. 3) could indicate that the repair tissue made by the chondrocytes in the NSP-PCL scaffold is more comparable to healthy hyaline cartilage in terms of matrix protein composition and elastic properties than that made by the Chondro-Gide® scaffold.

The histological scoring shows that the NSP-PCL scaffolds score significantly higher than the Chondro-Gide® scaffold in the categories "surface regularity" and "structural integrity;" however, none of the other categories showed significant differences. Although the beginning of a zonal stratification could be observed in a few of the samples (Fig. 12b), this was not achieved in full in any of the repaired cartilage. It is also clear from the sketch of the defects (Fig. 14) that a satisfactory level of repair in the center of the defects was not achieved in any treatment group. Even though Maehara et al. [18] found no significant difference in histological scoring when comparing cartilage repair in rabbits after 12 and 24 weeks, the lack of central repair could be attributed to the relatively short observational period (13 weeks).

The microenvironmental mechanics of a tissue or implant are capable of directing the development of cartilage. A scaffold with a very low stiffness will promote the formation of fibroblasts or neurons, while a scaffold with a

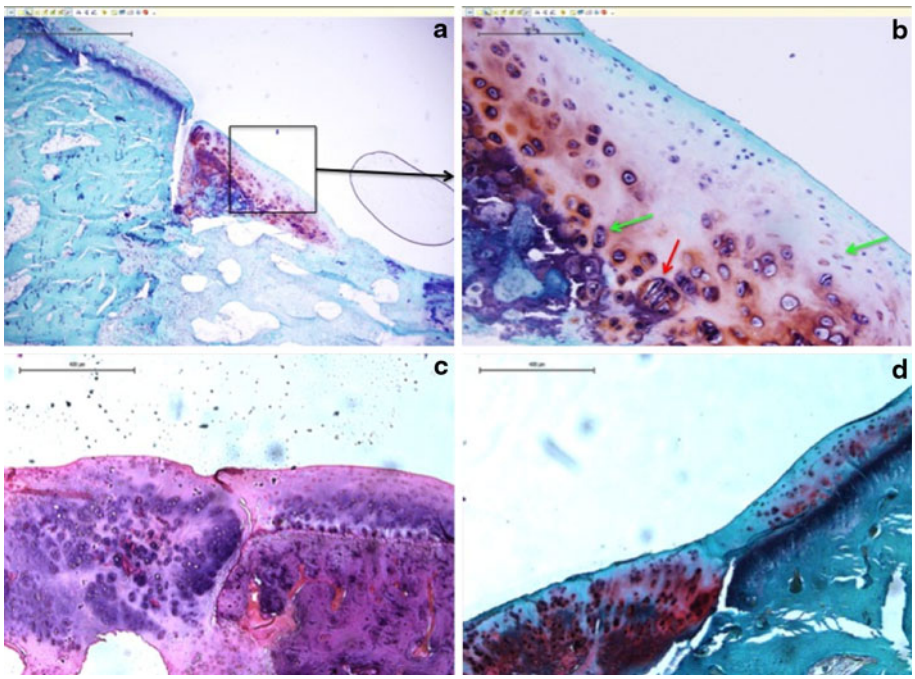

Fig. 12 **a** and **b** are high magnification micrographs of a knee treated with NSP-PCL/cells, and **c** and **d** are of two different knees treated with NSP-PCL/empty. The micrographs are taken from level 3 of the defect. **a** ×4 magnification of the transition zone between healthy cartilage and repair tissue. It is clearly shown as a tear in the surface. This is an artifact due to the embedding process. The *bar* is 800 μm. **b** ×20 magnification of the *squared area* of Fig. 12a. The *green arrows* show chondrocytes and the *red arrow* shows a cluster of chondrocytes. The repair tissue has a strong resemblance to normal hyaline cartilage, and though not yet achieved, the beginning of a zonal stratification can be seen. The *bar* is 150 μm. **c** and **d** HE and safranin-*O* stained ×4 magnification micrographs of the transition zone between healthy (on the *right*) and repair cartilage (on the *left*) on two different knees treated with the NSP-PCL scaffold without cells. *Bars* are 400 μm. In **c,** no apparent order to the arrangement of the chondrocytes is found; however, in **d,** the beginning of the zonal stratification is clearly seen in the repair tissue

high stiffness will promote the formation of bone [6, 8]. Due to relatively low stiffness of the lyophilized structure, the high stiffness of the plotted PCL scaffold and slow degradation properties, PCL scaffolds appear to be very suitable for hyaline cartilage repair in vivo. A study by Lam et al. [17] reported that the by-products of PCL degradation are non-toxic and are metabolized and eliminated via natural pathways. They found a mass loss of 2.13% and no change in stiffness (of the plotted scaffold) after 6 months of degradation in PBS. This suggests that implanted NSP-PCL scaffolds will maintain their mechanical stability and thus the mechanical microenvironment, which is in coherence with the results from our study that the NSP-PCL scaffold scores higher in structural integrity than the Chondro-Gide® scaffold. In a clinical setting, the stability of the NSP-PCL scaffold also provides the surgeon with a scaffold that is very easy to handle, thus limiting the risk of damaging the scaffold, and since the scaffold is press fitted into the defect, the need to suture the scaffold in place is eliminated.

In this study, we used an osteochondral drill hole defect, which means that bone marrow-derived mesenchymal stem cells (MSC) would be available in the defect. A possible explanation to the fact that we did not find a difference between NSP-PCL/cells and NSP-PCL/empty could be the migration of MSC's into the scaffold. The fact that NSP-PCL/cells did not score significantly higher in the category "cellular morphology" than NSP-PCL/empty could mean that the NSP-PCL scaffold facilitates the differentiation of the migrating MSC's into a hyaline–cartilage-like tissue, thus making chondrocytes seeded on the scaffold prior to implantation redundant. This means that when repairing an osteochondral defect, no prior chondrocyte biopsy is needed, making the treatment a one-step procedure, and thus eliminating donor site morbidity and providing a more cost-effective treatment.

Limitations of this study include the fact that the repaired defect is acute rather than chronic, which makes the model less comparable to human defects [27]. We did not include a treatment group in which the defects were left untreated because it has been shown that critical size defects do not heal well [18, 21]. In the in vitro part of the study, we investigated the gene expression of aggrecan, sox9, collagen types 1 and 2; however, the only way to be completely sure that the higher expression of a gene actually translates

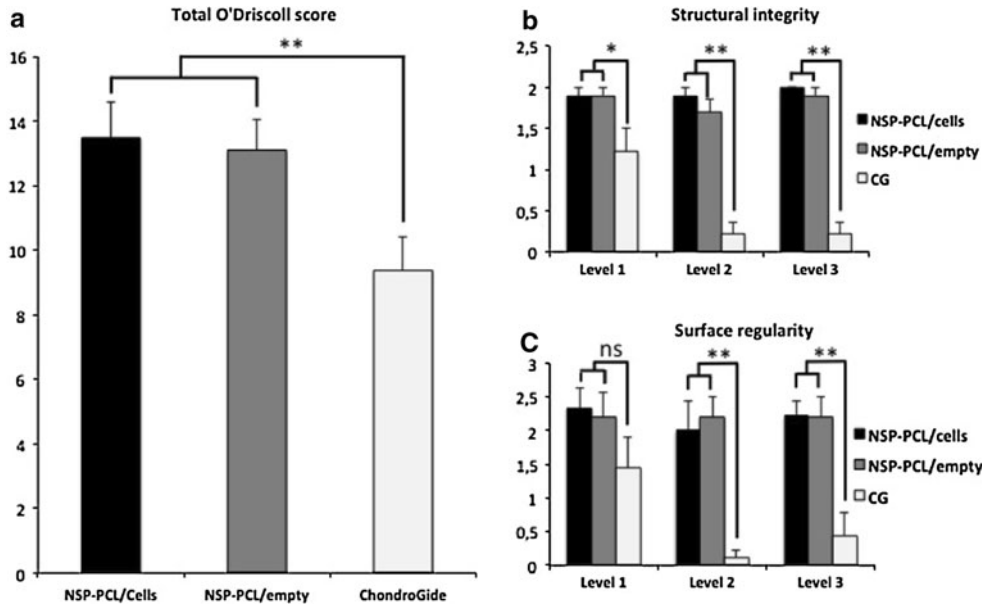

Fig. 13 **a** The NSP-PCL scaffold scored significantly higher in total O'Driscoll score than the Chondro-Gide scaffold; however, autologous cell seeding prior to implantation of the NSP-PCL scaffold had no effect on cartilage repair (*Y* axis is total O'Driscoll score. Maximal achievable score is 24). **b** Comparison of the structural integrity of the three levels and of each treatment. The NSP-PCL scaffolds scored significantly higher than the Chondro-Gide scaffolds on all three levels in the category "structural integrity" (*Y* axis is the score. Maximal achievable value is 2). **c** Comparison of the surface regularity of the three levels and of each treatment. No significant difference was found between the treatments on level 1 (Maximal achievable value is 3). (All *error bars* are SEM. $*P < 0.013$; $**P < 0.002$. *ns* not significant)

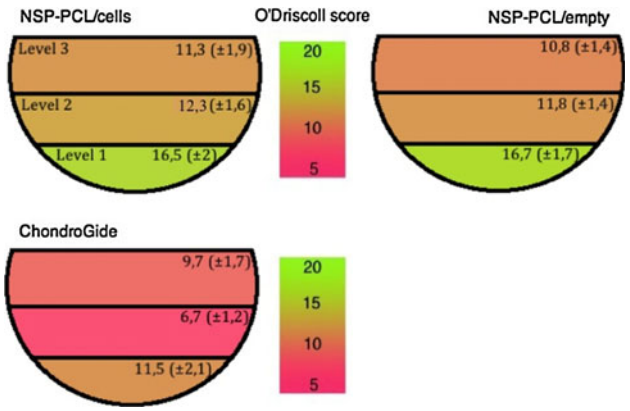

Fig. 14 A schematic overview of the cartilage repair of the defects by level. The numbers shown are the total scores of each level of each treatment (±SEM)

into an increased production of protein, is to perform a protein analysis. This was not performed in this study. The animal model used also has some limitations. Because the thickness of rabbit articular cartilage ranges between 0.25 and 0.75 mm compared to 2.2–4.3 mm in humans, it is very difficult to create a full-thickness cartilage defect [10]. The osteochondral drill hole defect supplies the defect with bone marrow-derived MSC's, which does improve spontaneous repair of the articular cartilage [27].

In this study, we applied the Chondro-Gide® scaffold using 3rd generation ACI, or MACI where autologous chondrocytes are seeded onto a polymer matrix and glued into a defect [1, 14]. When used in a clinical setting as a MACI scaffold, the Chondro-Gide® scaffold is glued into a full-thickness chondral defect; however, due to the limitations of the rabbit model, we used an osteochondral defect. One could argue that the treatment tested in this study is a hybrid of the matrix-assisted ACI technique and the membrane-covered microfracture or AMIC technique. Since the Chondro-Gide® scaffold is applied to both techniques in a clinical setting, we do not find this to be a significant limitation to the study.

Other studies using PCL scaffolds have reported a good restoration of the subchondral bone [12, 19, 29]; however, no samples in any of the three treatment groups showed a restoration of the subchondral bone. This could be due to the relatively short observational period; however, it could also be due the fact that the porosity of the NSP-PCL scaffold is designed to promote cartilage ingrowth and not bone ingrowth. The limitations of the rabbit model dictate that the scaffold has to be used as an osteochondral plug; however, in future studies, the NSP-PCL scaffold should be tested in a larger animal model, in a full-thickness chondral defect and for a longer period of time.

Conclusion

The novel NSP-PCL scaffold was successfully tested for articular cartilage repair in a rabbit model. The defects treated with the NSP-PCL scaffold had a good surface regularity and an excellent structural integrity compared to the clinically used Chondro-Gide® scaffold. Based on these results, we suggest that the NSP-PCL scaffold is superior to Chondro-Gide® for hyaline cartilage repair in an osteochondral rabbit model. The improved chondrocytic differentiation can potentially produce more hyaline cartilage during clinical cartilage repair. We found that the NSP-PCL scaffold performed equally well cell-free as when cells were added to the scaffold. This provides the possibility of using the scaffold in a cell-free, one-step procedure.

Acknowledgements The authors thank Anna Bay Nielsen, Anette Baatrup, Jane Pauli, Jonas Jensen from the Orthopaedic Research Laboratory and Steffen Ringgaard from the MR-Research Centre at Aarhus University Hospital for expert technical assistance. Funding was provided from the Individualized Musculoskeletal Regeneration and Reconstruction Network. Project no. 8415, grant holder: Cody Eric Bünger.

References

1. Behrens P, Bitter T, Kurz B, Russlies M (2006) Matrix-associated autologous chondrocyte transplantation/implantation (MACT/MACI): 5-year follow-up. Knee 13:194–202
2. Behrens P, Bosch U, Bruns J, Erggelet C, Esenwein SA, Gaissmaier C, Krackhardt T, Lohnert J, Marlovits S, Meenen NM, Mollenhauer J, Nehrer S, Niethard FU, Noth U, Perka C, Richter W, Schafer D, Schneider U, Steinwachs M, Weise K (2004) Indications and implementation of recommendations of the working group "tissue regeneration and tissue substitutes" for autologous chondrocyte transplantation (ACT). Z Orthop Ihre Grenzgeb 142:529–539
3. Benthien JP, Behrens P (2010) Autologous matrix-induced chondrogenesis (AMIC). A one-step procedure for retropatellar articular resurfacing. Acta Orthop Belg 76:260–263
4. Brittberg M, Lindahl A, Nilsson A, Ohlsson C, Isaksson O, Peterson L (1994) Treatment of deep cartilage defects in the knee with autologous chondrocyte transplantation. N Engl J Med 331:889–895
5. Buckwalter JA, Mankin HJ (1998) Articular cartilage: degeneration and osteoarthritis, repair, regeneration, and transplantation. Instr Course Lect 47:487–504
6. Discher DE, Janmey P, Wang YL (2005) Tissue cells feel and respond to the stiffness of their substrate. Science 310:1139–1143
7. Ehlers EM, Fuss M, Rohwedel J, Russlies M, Kuhnel W, Behrens P (1999) Development of a biocomposite to fill out articular cartilage lesions. Light, scanning and transmission electron microscopy of sheep chondrocytes cultured on a collagen I/III sponge. Ann Anat 181:513–518
8. Engler AJ, Sen S, Sweeney HL, Discher DE (2006) Matrix elasticity directs stem cell lineage specification. Cell 126:677–689
9. Haddo O, Mahroof S, Higgs D, David L, Pringle J, Bayliss M, Cannon SR, Briggs TW (2004) The use of chondrogide membrane in autologous chondrocyte implantation. Knee 11:51–55
10. Hall FM, Wyshak G (1980) Thickness of articular cartilage in the normal knee. J Bone Jt Surg Am 62:408–413
11. Hattori T, Muller C, Gebhard S, Bauer E, Pausch F, Schlund B, Bosl MR, Hess A, Surmann-Schmitt C, von der Mark H, de Crombrugghe B, von der Mark K (2010) SOX9 is a major negative regulator of cartilage vascularization, bone marrow formation and endochondral ossification. Development 137:901–911
12. Ho ST, Hutmacher DW, Ekaputra AK, Hitendra D, Hui JH (2010) The evaluation of a biphasic osteochondral implant coupled with an electrospun membrane in a large animal model. Tiss Eng Part A 16:1123–1141
13. Hunziker EB (2002) Articular cartilage repair: basic science and clinical progress. A review of the current status and prospects. Osteoarthr Cartil 10:432–463
14. Kon E, Filardo G, Condello V, Collarile M, Di Martino A, Zorzi C, Marcacci M (2011) Second-generation autologous chondrocyte implantation: results in patients older than 40 years. Am J Sports Med 39:1668–1675
15. Krishnan SP, Skinner JA, Carrington RW, Flanagan AM, Briggs TW, Bentley G (2006) Collagen-covered autologous chondrocyte implantation for osteochondritis dissecans of the knee: 2–7-year results. J Bone Jt Surg Br 88:203–205
16. Kubo S, Cooper GM, Matsumoto T, Phillippi JA, Corsi KA, Usas A, Li G, Fu FH, Huard J (2009) Blocking vascular endothelial growth factor with soluble Flt-1 improves the chondrogenic potential of mouse skeletal muscle-derived stem cells. Arthritis Rheum 60:155–165
17. Lam CX, Hutmacher DW, Schantz JT, Woodruff MA, Teoh SH (2009) Evaluation of polycaprolactone scaffold degradation for 6 months in vitro and in vivo. J Biomed Mater Res A 90:906–919
18. Maehara H, Sotome S, Yoshii T, Torigoe I, Kawasaki Y, Sugata Y, Yuasa M, Hirano M, Mochizuki N, Kikuchi M, Shinomiya K, Okawa A (2010) Repair of large osteochondral defects in rabbits using porous hydroxyapatite/collagen (HAp/Col) and fibroblast growth factor-2 (FGF-2). J Orthop Res 28:677–686
19. Martinez-Diaz S, Garcia-Giralt N, Lebourg M, Gomez-Tejedor JA, Vila G, Caceres E, Benito P, Pradas MM, Nogues X, Ribelles JL, Monllau JC (2010) In vivo evaluation of 3-D polycaprolactone scaffolds for cartilage repair in rabbits. Am J Sports Med 38:509–519
20. Minas T, Nehrer S (1997) Current concepts in the treatment of articular cartilage defects. Orthopedics 20:525–538
21. Mrosek EH, Schagemann JC, Chung HW, Fitzsimmons JS, Yaszemski MJ, Mardones RM, O'Driscoll SW, Reinholz GG (2010) Porous tantalum and poly-epsilon-caprolactone biocomposites for osteochondral defect repair: preliminary studies in rabbits. J Orthop Res 28:141–148
22. Ng KW, Hutmacher DW, Schantz JT, Ng CS, Too HP, Lim TC, Phan TT, Teoh SH (2001) Evaluation of ultra-thin poly(epsilon-caprolactone) films for tissue-engineered skin. Tiss Eng 7:441–455
23. Niemeyer P, Pestka JM, Kreuz PC, Erggelet C, Schmal H, Suedkamp NP, Steinwachs M (2008) Characteristic complications after autologous chondrocyte implantation for cartilage defects of the knee joint. Am J Sports Med 36:2091–2099
24. O'Driscoll SW, Keeley FW, Salter RB (1988) Durability of regenerated articular cartilage produced by free autogenous periosteal grafts in major full-thickness defects in joint surfaces under the influence of continuous passive motion. A follow-up report at 1 year. J Bone Jt Surg Am 70:595–606
25. Pfaffl MW, Tichopad A, Prgomet C, Neuvians TP (2004) Determination of stable housekeeping genes, differentially regulated target genes and sample integrity: best keeper–excel-based tool using pair-wise correlations. Biotechnol Lett 26:509–515
26. Pitt CG, Gratzl MM, Kimmel GL, Surles J, Schindler A (1981) Aliphatic polyesters II. The degradation of poly (DL-lactide), poly

(epsilon-caprolactone), and their copolymers in vivo. Biomaterials 2:215–220
27. Reinholz GG, Lu L, Saris DB, Yaszemski MJ, O'Driscoll SW (2004) Animal models for cartilage reconstruction. Biomaterials 25:1511–1521
28. Russlies M, Ruther P, Koller W, Stomberg P, Behrens P (2003) Biomechanical properties of cartilage repair tissue after different cartilage repair procedures in sheep. Z Orthop Ihre Grenzgeb 141:465–471
29. Shao XX, Hutmacher DW, Ho ST, Goh JC, Lee EH (2006) Evaluation of a hybrid scaffold/cell construct in repair of high-load-bearing osteochondral defects in rabbits. Biomaterials 27:1071–1080
30. Steinert AF, Ghivizzani SC, Rethwilm A, Tuan RS, Evans CH, Noth U (2007) Major biological obstacles for persistent cell-based regeneration of articular cartilage. Arthritis Res Ther 9:213
31. Woodward SC, Brewer PS, Moatamed F, Schindler A, Pitt CG (1985) The intracellular degradation of poly(epsilon-caprolactone). J Biomed Mater Res 19:437–444
32. Yamashita S, Andoh M, Ueno-Kudoh H, Sato T, Miyaki S, Asahara H (2009) Sox9 directly promotes Bapx1 gene expression to repress Runx2 in chondrocytes. Exp Cell Res 315:2231–2240